Article:

Huang, J, Yang, P, Wan, B et al. (1 more author) (2022) KDLPCCA-Based Projection for Feature Extraction in SSVEP-Based Brain-Computer Interfaces. Journal of Shanghai Jiaotong University (Science), 27 (2). pp. 168-175. ISSN 1007-1172

https://doi.org/10.1007/s12204-021-2387-0

KDLPCCA-Based Projection for Feature Extraction in SSVEP-Based Brain-Computer Interfaces

HUANG Jiayang[1](黄嘉阳), *YANG Pengfei*[1*] (杨鹏飞), *WAN Bo*[1](万波), *ZHANG Zhiqiang*[2]（张志强）

(1. School of Computer Science and Technology, Xidian University, Xi'an 710071, China;

2. School of Electronic and Electrical Engineering, University of Leeds, Leeds LS2 9JT, UK.)

- **Abstract:** An electroencephalogram (EEG) signal projection using kernel discriminative locality preserving canonical correlation analysis (KDLPCCA)-based correlation with steady-state visual evoked potential (SSVEP) templates for frequency recognition is presented in this paper. With KDLPCCA, not only a non-linear correlation but also local properties and discriminative information of each class sample are considered to extract temporal and frequency features of SSVEP signals. The new projected EEG features are classified with classical machine learning algorithms, namely, K-nearest neighbors (KNNs), naive Bayes, and random forest classifiers. To demonstrate the effectiveness of the proposed method, 16-channel SSVEP data corresponding to 4 frequencies collected from 5 subjects were used to evaluate the performance. Compared with the state of the art canonical correlation analysis (CCA), experimental results show significant improvements in classification accuracy and information transfer rate (ITR), achieving 100% and 240 bits/min with 0.5s sample block. The superior performance demonstrates that this method holds the promising potential to achieve satisfactory performance for high-accuracy SSVEP-based brain-computer interfaces.

Key words: steady-state visual evoked potential, brain-computer interface, feature extraction, kernel discriminative locality preserving canonical correlation analysis

CLC number: R 318, TN 911.7 **Document code:** A

Nomenclature

a_e—Projection vectors of EEG signals

$\boldsymbol{a}_r$—Projection vectors of the reference signals

A_e—Eigenvectors of EEG signals

A_r—Eigenvectors of reference signals

B—One matrix

c—Number of channels

C_1—A term in the objective function

C_2—A term in the objective function

C_3—A term in the objective function

C_4—A term in the objective function

d—Number of eigenvalues

D_e—Diagonal matrix of EEG signals from the same stimulus frequency

$\widetilde{D}_e$—Diagonal matrix of EEG signals from different stimulus frequencies

D_r—Diagonal matrix of reference signals from the same stimulus frequency

$\widetilde{D}_r$—Diagonal matrix of reference signals from different stimulus frequencies

$\boldsymbol{e}_i$—Concatenated EEG signals matrix of one block

e^{te}—A new EEG feature vector for test

e_k^{tr}—Concatenated EEG signals matrix from the training set

E—Segmented EEG signals matrix

f—Base frequency

f_k—Label set

h—Number of harmonics

i—Index of features

I—Identity matrix

i, j—Index of features

k—Index of frequencies

K—Number of stimulus frequencies

K_e—Gram matrix of EEG signals

L_e—Laplacian matrix of EEG signals from the same stimulus frequency

$\tilde{L}_e$—Laplacian matrix of EEG signals from different stimulus frequencies

L_r—Laplacian matrix of reference signals from the same stimulus frequency

$\tilde{L}_r$—Laplacian matrix of reference signals from different stimulus frequencies

M—A centering matrix

m—Dimensions of X_e

n—Dimensions of X_r

n_{ITR}—Information transfer rate (ITR)

N—Total number of sample blocks of all stimulus frequencies collected from one subject

p—Dimensions of Ψ_e

P—Classification accuracy

q—Dimensions of Ψ_r

r_i—Concatenated reference signals matrix of one block

R—Segmented reference signals matrix

s^{te}—Projected EEG feature vector of a new EEG feature vector

s_k^{tr}—Projected EEG feature vector of an EEG feature vector from the training set

S—Sampling rate

S_{tr}—Training set

T—Number of sampling points of a sample block

w—Index of eigenvalues

X_e—Concatenated EEG signals matrix

X_r—Concatenated reference signals matrix

γ —Correlation coefficient of a_e and $\boldsymbol{a}_r$

σ_e—Mean of all mapped EEG signals

ζ —Balancing parameter

θ_{ij}^{e} —L2-norm distance of two mapped EEG signals

Θ_e—Similarity matrix of EEG signals from the same stimulus frequency

$\tilde{\Theta}_e$—Similarity matrix of EEG signals from different stimulus frequencies

Θ_r—Similarity matrix of reference signals from the same stimulus frequency

$\tilde{\Theta}_r$—Similarity matrix of reference signals from different stimulus frequencies

λ_w —Generalized eigenvalues

μ_e—Width of the EEG Gaussian kernel

μ_r—Width of the reference Gaussian kernel

$\bar{\psi}_{\mathrm{e}}$ —Mean vector of $\psi_e(\boldsymbol{e}_i)(i = 1, 2, \ldots, N)$

Ψ_e—Mapped EEG signals matrix

Ψ_r—Mapped reference signals matrix

ω_e—Projection vector of EEG signals

ω_r—Projection vector of reference signals

Subscripts

e—EEG signals

r—Reference signals

te—Test set

tr—Training set

0 Introduction

Brain-computer interfaces (BCIs) provide a direct pathway for users interacting with external interfaces through brain activities independent from the neuromuscular pathways[1]. Among the various brain-sensing modalities, electroencephalography (EEG)-based BCIs, which have relatively short-time constants, can function in most environments, and require relatively simple and inexpensive equipment, are widely adopted as a new non-muscular communication and control interface[2]. For instance, steady-state visual evoked potentials (SSVEPs)[3], slow cortical potentials[4], P300 evoked potentials[5], event-related (de)synchronization[6], and mental tasks[7] are several commonly used non-invasive electrophysiological signal sources for control signals in BCI systems. Particularly, SSVEP-based BCIs provide the highest classification accuracy[8], information transfer rate (ITR)[9], and signal-to-noise ratio (SNR)[10]. A major challenge of SSVEP-based BCI research is how to improve the classification accuracy under the short response time, which would ensure that BCI transfers accurate control commands in time for practical applications[11].

[1]To improve the classification accuracy of frequency recognition, the key is to precisely describe the features of EEG induced by SSVEP. Varieties of methods such as discrete Fourier transform[12], short-time Fourier transform[13], minimum energy combination (MEC)[14], and maximum contrast combination (MCC) [15], have been proposed and demonstrated to be efficient SSVEP feature extraction methods.

Received: 2020-07-13 **Accepted:** 2020-10-10

Foundation item: the Natural Science Foundation of China (Nos. 61702395 and 61972302), and the Science and Technology Projects of Xi'an, China (No. 201809170CX11JC12)

* **E-mail:** pfyang@xidian.edu.cn

Among them, canonical correlation analysis (CCA), which uses the synthetically constructed SSVEP references consisting of sinusoidal signals to improve the detection accuracy, is the most widely used in SSVEP-based BCI[16]. In addition, some extended CCA-based methods such as cluster analysis of CCA coefficient (CACC)[17], individual template-based CCA (IT-CCA)[18], and multi-set CCA (MsetCCA)[19], have been proposed recently to improve the performance of frequency recognition. All of the existing methods only utilize the linear correlation between SSVEP signals and the reference signals. EEG signals induced by SSVEP, as a type of physiological electrical signals, have the non-linear characteristic. To be specific, based on the generation process of SSVEP signals, the response signals are transmitted to the surface of the scalp through the skull and they are mixed multiple times during the transmission[20]. So the correlation between SSVEP signals and the reference signals should not only be linear but also be non-linear. Therefore, the non-linear correlation between SSVEP signals and the reference signals should also be considered to fully describe the linear and non-linear temporal and frequency features of SSVEP signals.

Besides, for most SSVEP-based BCI applications, it is desirable for the processing to occur in real-time. In other words, the feature vectors should be extracted from small sample blocks segmented from incoming signal samples and be accurately translated to device commands. It is required that even with small amounts of sampling points, the temporal and frequency features of SSVEP signals should be fully described.

To resolve these problems, an EEG feature projection using kernel discriminative locality preserving canonical correlation analysis (KDLPCCA)-based correlation with SSVEP templates for frequency recognition is proposed in this paper. With KDLPCCA, not only a non-linear correlation but also local properties and discriminative information of each class sample are considered to fully describe the temporal and frequency features of SSVEP signals. The new projected EEG features are classified with classical machine learning algorithms, namely, K-nearest neighbors (KNNs), naive Bayes and random forest classifiers. The effectiveness of the proposed method was demonstrated with 16-channel SSVEP data corresponding to 4 frequencies (6Hz, 7.5Hz, 8.5Hz, and 10Hz) collected from 5 subjects. The promising experimental results show that the proposed method can achieve satisfactory performance for high-accuracy SSVEP-based BCIs.

The main contributions of KDLPCCA for SSVEP-based BCI are as follows. On one hand, KDLPCCA significantly increased the classification accuracy and ITR, thus making SSVEP-based BCI highly efficient. On the other hand, KDLPCCA can fully describe temporal and frequency features from SSVEP signals even with small sample blocks, thus increasing the classification accuracy and ITR of small sample blocks data, which makes SSVEP-based BCI system with fast response and high speed.

1 Methodology

In this paper, we employed a feature extraction method KDLPCCA for SSVEP detection and recognition. KDLPCCA[21] is an expansion of kernel CCA (KCCA)[22] combining with discriminative locality preserving CCA (DLPCCA)[23] to measure the linear and non-linear correlation between SSVEP EEG and reference signals. Therefore, KDLPCCA attempts to find a pair of projection vectors $\boldsymbol{a}_e$ and $\boldsymbol{a}_r$ by maximizing the correlation γ between SSVEP EEG and reference signals, which considers not only local structures but also class information. The optimization problem for correlation coefficient γ can be expressed as

$$\left(\boldsymbol{a}_{\mathrm{e}},\boldsymbol{a}_{\mathrm{r}}\right)=\arg\max_{\boldsymbol{a}_{\mathrm{e}},\boldsymbol{a}_{\mathrm{r}}}\gamma=\arg\max_{\boldsymbol{a}_{\mathrm{e}},\boldsymbol{a}_{\mathrm{r}}}\frac{\boldsymbol{a}_{\mathrm{e}}^{\mathrm{T}}\left(\boldsymbol{C}_1-\zeta\boldsymbol{C}_2\right)\boldsymbol{a}_{\mathrm{r}}}{\sqrt{\boldsymbol{a}_{\mathrm{e}}^{\mathrm{T}}\boldsymbol{C}_3\boldsymbol{a}_{\mathrm{e}}}\sqrt{\boldsymbol{a}_{\mathrm{r}}^{\mathrm{T}}\boldsymbol{C}_4\boldsymbol{a}_{\mathrm{r}}}}. \tag{1}$$

The terms C_1, C_2, C_3, C_4 are defined in equation (11)-(14) presented in the following parts. And the specific details of KDLPCCA-based projection for feature extraction will be presented as follows.

1.1 Constructing Reference Signals

Supposing that EEG signals of one subject are collected from c channels at K frequencies, and EEG signals are first segmented into sample blocks as $\boldsymbol{E}\in\mathbb{R}^{c\times T}$, where T is the number of sampling points of a sample block. The reference signals $\boldsymbol{R}\in\mathbb{R}^{2h\times T}$ are constructed as[16]

$$\boldsymbol{R}=\begin{bmatrix} r_1(t)\\ \vdots\\ r_{2h}(t)\end{bmatrix}=\begin{bmatrix} sin(2\pi f t)\\ cos(2\pi f t)\\ \vdots\\ sin(2h\pi f t)\\ cos(2h\pi f t)\end{bmatrix}, t=\frac{1}{S},\frac{2}{S},\dots,\frac{T}{S}, \tag{2}$$

where h is the number of harmonics, f is the base frequency, and S is the sampling rate. Then, the c rows of $\boldsymbol{E}$ are concatenated as a row, obtaining$\boldsymbol{e}_i\in\mathbb{R}^{c\times T}, i=1,2,\dots,N$. In the same manner, $\boldsymbol{R}$ are concatenated as$\boldsymbol{r}_i\in\mathbb{R}^{2h\times T}, i=1,2,\dots,N$. Hence, we obtain $\boldsymbol{X}_e=[\boldsymbol{e}_1,\boldsymbol{e}_2,\dots,\boldsymbol{e}_N]\in\mathbb{R}^{m\times N}$ for EEG signals, where $m=cT$, and $\boldsymbol{X}_r=[\boldsymbol{r}_1,\boldsymbol{r}_2,\dots,\boldsymbol{r}_N]\in\mathbb{R}^{n\times N}$ for reference signals, where$n=2hT$, N denotes the total number of sample blocks of all stimulus frequencies collected from one subject.

1.2 KDLPCCA-Based Projection for Feature Extraction

Next, KDLPCCA-based projection is applied for SSVEP signals feature extraction. By applying a kernel trick[22] for X_e and X_r, $\Psi_e = (\psi_e(e_1), \psi_e(e_2), \dots, \psi_e(e_N)) \in \mathbb{R}^{p\times N}$ and $\Psi_r = (\psi_r(r_1), \psi_r(r_2), \dots, \psi_r(r_N)) \in \mathbb{R}^{q\times N}$ are first obtained in the mapped Hilbert space, where p and q are the dimensions of EEG and reference feature vectors in the Hilbert space respectively. Then we compute the similarity matrices $\Theta_e = \{\Theta_{ij}^e\}_{i,j=1}^N \in \mathbb{R}^{N\times N}$ and $\tilde{\Theta}_e = \{\tilde{\Theta}_{ij}^e\}_{i,j=1}^N \in \mathbb{R}^{N\times N}$ by calculating the similarities between samples of i-th and j-th stimulus frequencies from Ψ_e as[23]

$$\Theta_{ij}^e = \begin{cases} exp(-\theta_{ij}^e/\sigma_e), & \boldsymbol{e}_i \text{ and } \mathbf{e}_j \text{from the same frequency,} \\ 0, & \text{otherwise;} \end{cases} \tag{3}$$

$$\tilde{\Theta}_{ij}^e = \begin{cases} exp(-\theta_{ij}^e/\sigma_e), & \boldsymbol{e}_i \text{ and } \mathbf{e}_j \text{from different frequencies,} \\ 0, & \text{otherwise.} \end{cases} \tag{4}$$

θ_{ij}^{e} and σ_{e} are calculated as

$$\theta_{ij}^e = \|\psi_e(\boldsymbol{e}_i) - \psi_e(\boldsymbol{e}_j)\|^2 = (K_e)_{ii} - 2(K_e)_{ij} + (K_e)_{jj}, \tag{5}$$

$$\sigma_e = \frac{1}{N(N-1)} \sum_{i=1}^N \sum_{j=1}^N \theta_{ij}^e, \tag{6}$$

where $K_e \in \mathbb{R}^{N\times N}$ is the gram matrix and calculated as $(K_e)_{ij} = k_e(e_i, e_j) = \psi_e(e_i)^T \psi_e(e_j)$ with a kernel trick. And the similarity matrices Θ_r and $\tilde{\Theta}_r$ of Ψ_r are calculated in the same manner.

Considering local structures and the class information based on locality preserving projection (LPP) [24] to fully describe EEG features, Laplacian matrices $L_e \in \mathbb{R}^{N\times N}$ and $\tilde{L}_e \in \mathbb{R}^{N\times N}$ are calculated based on the similarity matrices as

$$L_e = D_e - \Theta_e \circ \Theta_e, \tag{7}$$

$$\tilde{L}_e = \tilde{D}_e - \tilde{\Theta}_e \circ \tilde{\Theta}_e, \tag{8}$$

where the symbol $\circ$ represents the Hadamard product.

The derivations of $D_e \in \mathbb{R}^{N\times N}$ and $\tilde{D}_e \in \mathbb{R}^{N\times N}$ are calculated with Θ_{ij}^e and $\tilde{\Theta}_{ij}^e$ in Eqs. (3) and (4):

$$D_e = \mathrm{diag}[\textstyle\sum_j (\Theta_{1j}^e)^2, \sum_j (\Theta_{2j}^e)^2, \dots, \sum_j (\Theta_{Nj}^e)^2], \tag{9}$$

$$\tilde{D}_e = \mathrm{diag}[\textstyle\sum_j (\tilde{\Theta}_{1j}^e)^2, \sum_j (\tilde{\Theta}_{2j}^e)^2, \dots, \sum_j (\tilde{\Theta}_{Nj}^e)^2]. \tag{10}$$

The same way operated in Eqs.(9) and (10), D_r and $\tilde{D}_r$ are calculated, thereby obtaining L_r and $\tilde{L}_r$ based on Eqs.(7) and (8).

Then the terms $\boldsymbol{C}_1, \boldsymbol{C}_2, \boldsymbol{C}_3, \boldsymbol{C}_4 \in \mathbb{R}^{N\times N}$ in Eq. (1) are defined as

$$\boldsymbol{C}_1 = \boldsymbol{M}\boldsymbol{K}_e\boldsymbol{M}(\boldsymbol{\Theta}_e \circ \boldsymbol{\Theta}_r)\boldsymbol{M}\boldsymbol{K}_r\boldsymbol{M}, \tag{11}$$

$$\boldsymbol{C}_2 = \boldsymbol{M}\boldsymbol{K}_e\boldsymbol{M}(\widetilde{\boldsymbol{\Theta}}_e \circ \widetilde{\boldsymbol{\Theta}}_r)\boldsymbol{M}\boldsymbol{K}_r\boldsymbol{M}, \tag{12}$$

$$\boldsymbol{C}_3 = \boldsymbol{M}\boldsymbol{K}_e\boldsymbol{M}(\boldsymbol{L}_e + \tilde{\boldsymbol{L}}_e)\boldsymbol{M}\boldsymbol{K}_e\boldsymbol{M} + \varepsilon_e\boldsymbol{M}\boldsymbol{K}_e\boldsymbol{M}, \tag{13}$$

$$\boldsymbol{C}_4 = \boldsymbol{M}\boldsymbol{K}_r\boldsymbol{M}(\boldsymbol{L}_r + \tilde{\boldsymbol{L}}_r)\boldsymbol{M}\boldsymbol{K}_r\boldsymbol{M} + \varepsilon_r\boldsymbol{M}\boldsymbol{K}_r\boldsymbol{M}, \tag{14}$$

where $\boldsymbol{M} = \boldsymbol{I} - \frac{1}{N}\boldsymbol{B}\boldsymbol{B}^T \in \mathbb{R}^{N\times N}$ is a centering matrix, $\boldsymbol{I} \in \mathbb{R}^{N\times N}$ is the identity matrix, and $\boldsymbol{B} = (1, \dots, 1)^T \in \mathbb{R}^N$.

Equation (1) can be transformed into a generalized eigenvalue problem as:

$$\begin{bmatrix} & (\boldsymbol{C}_1 - \zeta\boldsymbol{C}_2) \\ (\boldsymbol{C}_1 - \zeta\boldsymbol{C}_2)^T & \end{bmatrix}\begin{bmatrix}\boldsymbol{a}_e \\ \boldsymbol{a}_r\end{bmatrix} = \lambda\begin{bmatrix}\boldsymbol{C}_3 & \\ & \boldsymbol{C}_4\end{bmatrix}\begin{bmatrix}\boldsymbol{a}_e \\ \boldsymbol{a}_r\end{bmatrix}, \tag{15}$$

By solving Eq.(15), we obtain $\boldsymbol{A}_e = (\boldsymbol{a}_{e_1}, \boldsymbol{a}_{e_2}, \dots, \boldsymbol{a}_{e_d}) \in \mathbb{R}^{N\times d}$ and $\boldsymbol{A}_r = (\boldsymbol{a}_{r_1}, \boldsymbol{a}_{r_2}, \dots, \boldsymbol{a}_{r_d}) \in \mathbb{R}^{N\times d}$ by extracting the basis vector pairs $(\boldsymbol{a}_{e_w}, \boldsymbol{a}_{r_w})$ corresponding to the first d largest generalized eigenvalues $\lambda_w (w = 1, 2, \dots, d)$. Based on $\boldsymbol{A}_e$ and $\boldsymbol{A}_r$, the projection vectors $\boldsymbol{\omega}_e \in \mathbb{R}^{p\times d}$ and $\boldsymbol{\omega}_r \in \mathbb{R}^{q\times d}$ are calculated as:

$$\boldsymbol{\omega}_e = \boldsymbol{\Psi}_e\boldsymbol{M}\boldsymbol{A}_e, \tag{16}$$

$$\boldsymbol{\omega}_r = \boldsymbol{\Psi}_r\boldsymbol{M}\boldsymbol{A}_r. \tag{17}$$

With the projection $\boldsymbol{\omega}_e$, the projected EEG feature vector $\boldsymbol{s}^{\text{te}} \in \mathbb{R}^d$ of a new EEG feature vector $\boldsymbol{e}^{\text{te}} \in \mathbb{R}^p$ is calculated as

$$\boldsymbol{s}^{\text{te}} = \boldsymbol{\omega}_e^T\{\psi_e(\boldsymbol{e}^{\text{te}}) - \bar{\psi}_e\} = \boldsymbol{A}_e^T\boldsymbol{M}\left\{\boldsymbol{\Psi}_e^T\psi_e(\boldsymbol{e}^{\text{te}}) - \frac{1}{N}\boldsymbol{K}_e\boldsymbol{B}\right\}, \tag{18}$$

where $\bar{\psi}_e = \frac{1}{N}\boldsymbol{\Psi}_e\boldsymbol{B} \in \mathbb{R}^p$ is the mean vector of $\psi_e(\boldsymbol{e}_i)(i = 1, 2, \dots, N)$.

1.3 Classification for Frequency Recognition

Finally, with the KDLPCCA projected EEG features, the corresponding stimulation frequencies can be recognized by classification. Three classical machine learning algorithms, namely, KNNs [25], naive Bayes [26], and random forest classifiers [27], are applied in this work. The training set $\boldsymbol{S}_{\text{tr}} = \{(\boldsymbol{s}_k^{\text{tr}}, f_k)\}_{k=1}^{N_{\text{tr}}}$ is used to train the classifiers, and the class of a projected EEG feature vector $\boldsymbol{s}^{\text{te}}$ without label is estimated by the trained classifiers. $\boldsymbol{s}_k^{\text{tr}}$ is calculated from the $\boldsymbol{e}_k^{\text{tr}}$ in the same way as $\boldsymbol{s}^{\text{te}}$, and $f_k \in \{1, 2, 3, 4\}$ correspond to the 4 stimulus frequencies.

In this way, the classification of SSVEP signals is realized for each subject adaptively and efficiently, because KDLPCCA projected EEG features have the best linear and non-linear correlation with the reference signals.

2 Experiments and Results

2.1 Dataset Description

The dataset includes 16-channel EEG data sampled at 256Hz with 4 stimulus frequencies. Five healthy subjects (including 3 males and 2 females, aged from 22 to 26 years) with normal or corrected-to-normal vision, without any brain-related diseases, participated in this study. All subjects had the experience of using the SSVEP-based BCIs. Each participant was informed with the experimental procedure before the experiment.

This study designed an offline BCI experiment using an SSVEP BCI controller with 4 control commands stimulated by the light-emitting diode (LED) flashing at 4 frequencies (6Hz, 7.5Hz, 8.5Hz, 10Hz). According to the research of Herrmann [28], the response of SSVEP decreases as the stimulus frequency increases. As a result, compared to medium frequency (15—30Hz) and high frequency (>30Hz), SSVEP response stimulated by low frequencies (<15Hz) is the greatest. Therefore, we choose 4 different frequencies (6Hz, 7.5Hz, 8.5Hz, and 10Hz) from the low frequency range. For each subject, EEG data were collected 5 trials at each stimulus frequency, and the acquisition time was 20 s each trial. All 5 trials provide enough blocks to analyze the performance of KDLPCCA. Each trial started as subjects were asked to focus on the stimulus as soon as possible. Subjects were instructed to avoid eye blinks during the stimulation duration. There was a rest for 2 min between two consecutive trials.

The acquisition equipment used in this experiment is g.USBamp. EEG data were recorded at a sampling rate of 256 Hz. The usable bandwidth of the system was 0.15—200 Hz. According to the 10—20 standard system, 16 channels (Pz, PO3, PO4, O1, O2, Oz, O9, FP2, C4, C6, CP3, CP1, CPz, CP2, CP4, PO8, the ground electrode is FPz) signals were collected. Electrode impedances were kept below 10 kΩ during recording. A notch filter at 50 Hz was applied to remove the power-line noise. During the experiment, subjects were seated in a comfortable chair in a dimly lit and quiet room.

2.2 Experiment Design

In our experiment, first, multi-channel EEG signals were segmented into sample blocks with different sizes, then pre-processed by 5—40 Hz bandpass filtering, and normalized to zero mean and unit variance. The reference signals were generated according to 4 stimulus frequencies and the number of harmonics was specified as 3. Next, in the process of KDLPCCA-based projection, we adopted Gaussian kernel, i.e., $k_e(\boldsymbol{e}_i, \boldsymbol{e}_j) = exp(-\frac{\|e_i - e_j\|^2}{2\mu_e^2})$, $k_r(\boldsymbol{r}_i, \boldsymbol{r}_j) = exp(-\frac{\|r_i - r_j\|^2}{2\mu_r^2})$, where the kernel widths $\mu_e^2 = \mu_r^2 = 0.3536$.

To obtain the optimal regularization parameters of KDLPCCA, ε_{e} and ε_{r} were set as 0.001. And the balancing parameter ζ was set as 1.0. The number of dimensions of projected features is equal to the number of stimulus frequencies, that is $d = K$. For classification, the EEG signals were separated into training and test sets at a ratio of 75%. Thus a training set $\boldsymbol{S}_{\mathrm{tr}} = \{(\boldsymbol{s}_k^{\mathrm{tr}}, f_k)\}_{k=1}^{N_{\mathrm{tr}}}$ and a test set $\boldsymbol{S}_{\mathrm{te}} = \{\boldsymbol{s}_l^{\mathrm{te}}\}_{l=1}^{N_{\mathrm{te}}}$ were obtained. Three classical machine learning algorithms, namely, KNNs, naive Bayes, and random forest classifiers, were applied in our work. The training set $\boldsymbol{S}_{\mathrm{tr}}$ was used to train the classifiers, and the labels of the test set $\boldsymbol{S}_{\mathrm{te}}$ would be estimated.

2.3 Experiment Results and Analysis

The three classifiers with KDLPCCA-based projection are compared with CCA and the ones without KDLPCCA on classification accuracies and ITR [9]. ITR is the amount of information communicated per minute, and can be calculated as

$$n_{\mathrm{ITR}} = \frac{60}{T}\left[log_2(K) + P\,log_2(P) + (1-P)\,log_2\left(\frac{1-P}{K-1}\right)\right]. \tag{19}$$

where K is the number of frequencies, P is the classification accuracy, and T represents the required time for visual stimulation in each operation period. From the formula, we can see that when the classification accuracies (P) are fixed, as the sample block (T) increases, n_{ITR} decreases. Meanwhile, when the sample block (T) are fixed, n_{ITR} increases as the classification accuracy increases.

The SSVEP signals are segmented into sample blocks with sizes of 0.3s, 0.5s, 0.7s, 1s, 1.5s, and 2s. Overall, the classical classifiers (especially naive Bayes) with KDLPCCA projection outperforms CCA and the ones without KDLPCCA even with small sample blocks on classification accuracies and ITR, as is shown in Figs. 1 and 2 respectively. NB and RF denote naive Bayes and random forest classifiers respectively, and the error bar represents the standard deviation (SD). With different sample blocks, the performances on the stability of classification accuracies are compared among classifiers for KDLPCCA projected features and CCA, as shown in Fig. 3.

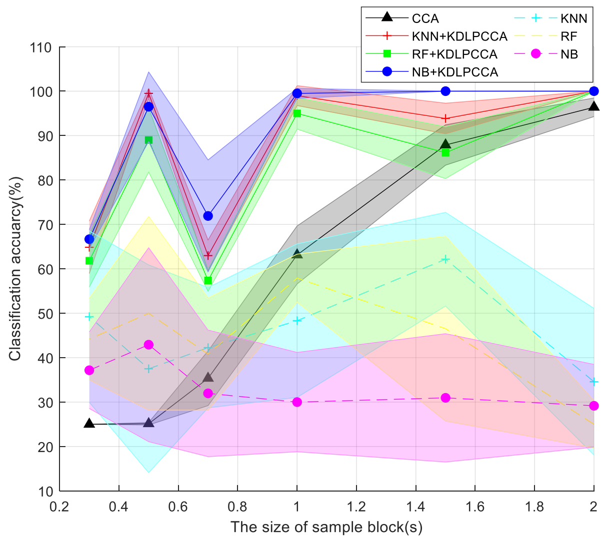

Fig. 1 Classification accuracies of classifiers with and without KDLPCCA-based projection and CCA

Figure 1 shows the classification accuracies of classifiers with and without KDLPCCA projection and CCA with different sizes of sample blocks among all subjects. The baseline CCA achieves an accuracy under 60% when the size of the sample block is smaller than 1 s. Meanwhile, with KDLPCCA-based projection, the naive Bayes classifier achieves an accuracy higher than 60%. When the sample block is larger than 1 s, classifiers with KDLPCCA projection have the accuracies greater than 90%, approaching 100%. With KDLPCCA-based projection, the naive Bayes classifier can achieve accuracy of 100% with 0.5 s, 1 s, 1.5 s, and 2 s sample block. Specifically, with 0.5 s sample block, the averaged accuracy across all subjects was 96.50±7.83%. Across individuals, the minimal and maximal classification accuracies were 82.5% and 100% respectively. Besides, classification accuracies of 1 s sample block range from 97.50% to 100%, with the average of 99.5% across all subjects. With sample blocks of all different sizes, classification for KDLPCCA projected features with three classifiers outperform baseline CCA. Furthermore, comparing the performance of classifiers with and without KDLPCCA-based projection, the classification accuracies of the three classical classifiers have greatly improved with the KDLPCCA projected features.

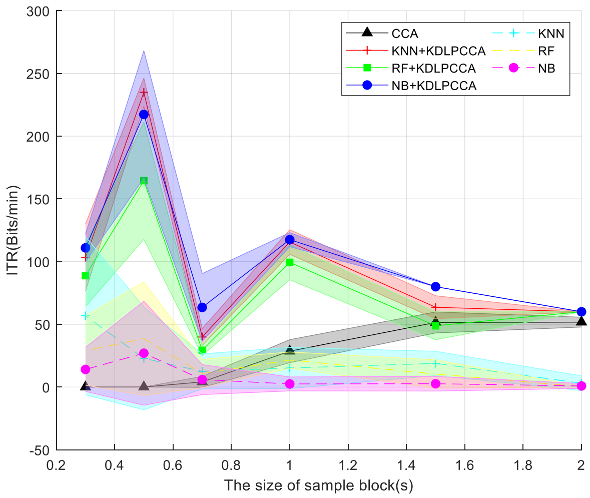

Fig. 2 ITR of classifiers with and without KDLPCCA-based projection and CCA.

Figure 2 illustrates the ITR of classifiers with and without KDLPCCA projection and CCA with different sizes of sample blocks among all subjects. All three classifiers for KDLPCCA projected features can achieve ITR up to 240 bits/min with 0.5 s sample block and 120 bits/min with 1 s sample block, which outperforms CCA with ITR under 60 bits/min. Classified by naive Bayes classifier, with 0.5 s sample block, the averaged ITR across all subjects is 217.29±50.78 bits/min. Across individuals, the minimal and maximal ITR are 126.43 bits/min and 240.00 bits/min respectively. Moreover, with 1s sample block, the average ITR of all subjects is 117.51±5.59 bits/min, and the minimum and maximum of ITR are 107.50 bits/min and 120.00 bits/min respectively. In addition, ITRs of 0.3s sample block range from 95.62 bits/min to 126.97 bits/min, with the average of 110.93 bits/min across all subjects. With sample blocks of different sizes, ITRs of all the classifiers have significantly improved with KDLPCCA-based projection.

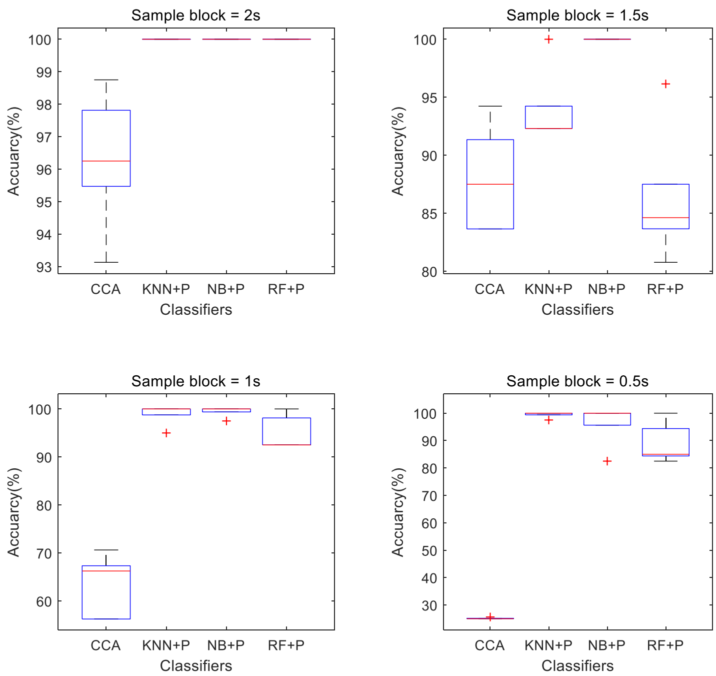

Fig. 3 Comparisons on the stability of classification accuracies between classifiers with KDLPCCA-based projection and CCA with sample blocks of 2 s, 1.5 s, 1 s, and 0.5 s

In Fig. 3, the performance on the stability of classification accuracies is compared among different subjects with sample blocks of 2 s, 1.5 s, 1 s, and 0.5 s. KNN+P, NB+P, and RF+P represent KNN, naive Bayes and random forest classifiers with KDLPCCA projection respectively. All classifiers with KDLPCCA projection has better stability on classification accuracies than CCA. With 2 s sample block, classifiers for KDLPCCA projected features of all subjects have a classification accuracy of 100%. Moreover, naive Bayes classifier with KDLPCCA projection has the best performance on stability with sample blocks greater than 1 s, while KNN outperforms other classifiers on classification accuracy stability with 0.5 s sample block. Superior performances demonstrate the proposed method can achieve satisfactory performance for high-accuracy SSVEP-based BCIs.

3 Discussion

The proposed feature extraction method, KDLPCCA, extracts not only a non-linear correlation but also local properties and discriminative information of each class sample to fully describe the temporal features of SSVEP signals. From the analysis with our datasets, KDLPCCA outperforms significantly in SSVEP segments with short response time in terms of classification accuracy and ITRs compared with CCA, as shown in Figs. 1 and 2. Besides, KDLPCCA shows less variability in classification accuracy compared with CCA, as Fig. 3 shows.

However, from the experiment analysis, it can be seen that there are still drawbacks to our proposed method. First, CCA is a classical feature extraction method with the advantage of calibration-free, whilst KDLPCCA is a method with the calibration process, which would produce massive computational costs for the training process. Also, KDLPCCA's classification accuracy and ITR have significant fluctuations between different sample blocks sizes compared with CCA. CCA is a feature extraction method with robustness. The classification accuracy and ITR of CCA increase as the sample block increases. But KDLPCCA considers linear and non-linear temporal and frequency features, which may be sensitive to other factors in temporal and frequency features that we need to further investigate. In other words, KDLPCCA is not as robust as CCA. Therefore, we would improve our method aiming at the problems in our future work.

Furthermore, to further verify the effectiveness of our method, SSVEP signals collected from subjects who are naive to SSVEP-based BCI should also be used for evaluation. And more data should be collected from more participants with more trials to evaluate the offline performance of the proposed method. Moreover, online experiments should also be implemented to evaluate the online performance of KDLPCCA. Based on the results of online experiments, we would apply this method to various practical SSVEP-based BCIs, such as cursor control and wheelchair control.

4 Conclusion

For practical SSVEP BCI applications, it is important to accurately recognize frequencies with small sample blocks. Most existing methods neglected non-linear characteristics of SSVEP signals. So the EEG signal projection using KDLPCCA-based correlation with SSVEP templates for frequency recognition is proposed to accurately describe EEG features for frequency recognition. The experimental results show a significant performance improvement in classification accuracies and ITR. The results demonstrated the proposed method holds great potential to achieve great performance for high-accuracy SSVEP-based BCIs.

Acknowledgement The authors would thank Mr. Bang Xiong and Mr. Cheng Fang for the assistance of the data acquisition in this study.

References

[1] WOLPAW J R, BIRBAUMER N, MCFARLAND D J, et al. Brain-computer interfaces for communication and control[J]. *Clinical Neurophysiology*, 2002, **113**(6):767-791.

[2] LOTTE F, BOUGRAIN L, CICHOCKI A, et al. A review of classification algorithms for EEG-based brain-computer interfaces: A 10 year update[J]. *Journal of Neural Engineering*, 2018, **15**(3):031005.

[3] WANG M, LI R, ZHANG R, et al. A wearable SSVEP-based BCI System for quadcopter control using head-mounted device[J]. *IEEE Access*, 2018, **6**(99):26789-26798.

[4] NEUMANN N, KÜBLER A, KAISER J, et al. Conscious perception of brain states: Mental strategies for brain-computer communication[J]. *Neuropsychologia*, 2003, **41**(8):1028-1036.

[5] CHAURASIYA R, LONDHE N, GHOSH S. A novel weighted edit distance-based spelling correction approach for improving the reliability of Devanagari script-based P300 speller system[J]. *IEEE Access*, 2016, **4**:8184-8198.

[6] SANTAMARIA L, JAMES C. Using brain connectivity metrics from synchrostates to perform motor imagery classification in EEG-based BCI systems[J]. *Healthcare Technology Letters*, 2018, **5**(3):88-93.

[7] CURRAN E, SYKACEK P, STOKES M, et al. Cognitive tasks for driving a brain-computer interfacing system: A pilot study[J]. *IEEE Transactions on Neural Systems and Rehabilitation Engineering*, 2004, **12**(1): 48-54.

[8] NAKANISHI M, WANG Y, WANG Y T, et al. Generating visual flickers for eliciting robust steady-state visual evoked potentials at flexible frequencies using monitor refresh rate[J]. *PLoS One*, 2014, **9**(6):e99235.

[9] CHEN X, CHEN Z, GAO S, et al. A high-ITR SSVEP-based BCI speller[J]. *Brain-Computer Interfaces*, 2014, **1**(3/4):181-191.

[10] DREYER A M, HERRMANN C S. Frequency-modulated steady-state visual evoked potentials: A new stimulation method for brain-computer interfaces[J]. *Journal of Neuroscience Methods*, 2015, **241**:1-9.

[11] ORTIZ-ROSARIO A, ADELI H. Brain-computer interface technologies: From signal to action[J]. *Reviews in the Neurosciences*, 2013, **24**(5):537-552.

[12] TREJO L J, ROSIPAL R, MATTHEWS B. Brain-computer interfaces for 1-D and 2-D cursor control: Designs using volitional control of the EEG spectrum or steady-state visual evoked potentials[J]. *IEEE Transactions on Neural Systems and Rehabilitation Engineering*, 2006, **14**(2):225-229.

[13] JIA D, DAI H, TAKASHIMA Y, et al. EEG processing in Internet of medical things using non-harmonic analysis: Application and evolution for SSVEP responses[J]. *IEEE Access*, 2019, **7**:11318-11327.

[14]TRIGUI O, ZOUCH W, BEN M. Anti-noise capability improvement of minimum energy combination method for SSVEP detection[J]. *International Journal of Advanced Computer Science and Applications*, 2016, **7**(9):393-401.

[15]ABU-ALQUMSAN M, PEER A. Advancing the detection of steady-state visual evoked potentials in brain－computer interfaces[J]. *Journal of Neural Engineering*, 2016, **13**(3):036005.

[16]LIN Z, ZHANG C, WU W, et al. Frequency recognition based on canonical correlation analysis for SSVEP-based BCIs[J]. *IEEE Transactions on Biomedical Engineering*, 2007, **54**(6):1172-1176.

[17]PORYZALA P, MATERKA A. Cluster analysis of CCA coefficients for robust detection of the asynchronous SSVEPs in brain-computer interfaces[J]. *Biomedical Signal Processing and Control*, 2014, **10**(mar.):201-208.

[18]BIN G, GAO X, WANG Y, et al. A high-speed BCI based on code modulation VEP[J]. *Journal of Neural Engineering*, 2011, **8**(2):025015.

[19]ZHANG Y, ZHOU G, JIN J, et al. Frequency recognition in SSVEP-based BCI using multiset canonical correlation analysis[J]. *International Journal of Neural Systems*, 2014, **24**(4):1450013

[20]BAILLET S, MOSHER J C, LEAHY R M. Electromagnetic brain mapping[J]. *IEEE Signal Processing Magazine*, 2001, **18**(6):14-30.

[21]SAWATA R, OGAWA T, HASEYAMA M. Novel audio feature projection using KDLPCCA-based correlation with EEG features for favorite music classification[J]. *IEEE Transactions on Affective Computing*, 2019, **10**(3):430-444.

[22]AKAHO S. A kernel method for canonical correlation analysis[EB/OL] (2007-02-14). https://arxiv.org/abs/cs/0609071.

[23]ZHANG X, GUAN N, LUO Z, et al. Discriminative Locality Preserving Canonical Correlation Analysis[M]// *Pattern recognition*. Berlin, Heidelberg: Springer, 2012: 341-349.

[24]HE X, NIYOGI P. Locality preserving projections[M]// *Advances in Neural Information Processing Systems*. Cambridge, USA: MIT Press, 2004.

[25]ARIS S A M, JALIL S Z A, BANI N A, et al. EEG features extraction and k-NN classification during eyes closed[C]// *2016 IEEE EMBS Conference on Biomedical Engineering and Sciences*. Kuala Lumpur, Malaysia: IEEE, 2016:679-684.

[26]RAKSHIT A, KHASNOBISH A, TIBAREWALA D N. A Naive Bayesian approach to lower limb classification from EEG signals[C]// *2016 2nd International Conference on Control, Instrumentation,*

Energy & Communication (CIEC). Kolkata, India: IEEE, 2016:140-144.

[27]BOSE S, RAMA V, WARANGAL N, et al. EEG signal analysis for Seizure detection using Discrete Wavelet Transform and Random Forest[C]// *2017 International Conference on Computer and Applications (ICCA)*. Doha, Qatar: IEEE, 2017:369-378.

[28]HERRMANN C S. Human EEG responses to 1-100 Hz flicker: Resonance phenomena in visual cortex and their potential correlation to cognitive phenomena[J]. *Experimental Brain Research*, 2001, **137**(3/4):346-353.